Simulation and experimental estimation of the free wavenumbers for helically grooved tubes

Milena Watanabe Bavaresco[1], Neil Ferguson[1], Claus Hessler Ibsen[2] and Atul Bhaskar[1]

[1] University of Southampton, Southampton SO17 1BJ, UK
[2] Vestas aircoil, Smed Hansens Vej 13, 6940 Lem, Denmark

Abstract. The dynamic characterisation of elastic tubes is relevant to many fields in the industry. They are a key component for many processes involving fluid flow, heating, or cooling, etc., where grooves are frequently introduced to alter flow, and thus enhance heat transfer. Thin-walled tubes with helical features have been previously studied numerically and analytically, but experimental observation is still missing. In this paper, the wave propagation characteristics of a cylindrical tube with helicoidal grooves are investigated experimentally. The Wave Finite Element method is applied to a 3D model of this structure and a correlation method is used on a physical tube to experimentally observe the splitting of the degenerate dispersion branch into two. As opposed to a tube without grooves, both numerical and experimental methods show that the tubes with helicoidal grooves possess two distinctive but closely valued bending wave branches in the dispersion curves. The effect of the grooves is also visible in the mode shapes of the tubes of finite length, which will also be presented, where bending modes become unrestricted to lying in a single preferential direction.

Keywords: Pipes, Helicoidal grooves, Wave propagation, Experimental estimation of wavenumbers.

1 Introduction

The characterisation of wave properties of mechanical structures has gained increased interest for topics such as damage detection, wave focusing and general understanding of the dynamic behavior of structures, to name a few. In this context, long slender structures with helical aspects have been analysed to identify existing propagating waves ([1-4]).

A characteristic effect of the helical geometry in the wave properties of these structures is that two distinctive flexural branches are visible in their dispersion curves. This contrasts to the two identical flexural branches related to degenerate modes occurring in orthogonal planes in an equivalent non-helical structure. This effect has been reported for helical waveguides in the form of beams through an analytical approach by Frikha [5], rods and wires through the Semi-Analytical Finite Element (SAFE) method in Tresseyde's work [3], through the Scaled Boundary Finite Element Method (SBFEM) in Liu's et al work [4], and for helical springs through the Wave Finite Element (WFE) method in Renno and Mace's work [6]. A similar phenomenon was observed for a non-helical but curved pipe in work of Demma et al. [7], in which a mode that is described by one dispersion curve for a straight pipe splits into two

dispersion curves in the curved pipe. Having observed this effect through these analytical and numerical investigations, this work is motivated by the need to experimentally observe the two distinctive flexural branches in a structure with helical features.

Among the existing experimental methods for the estimation of wavenumbers in one-dimensional waveguides, this paper focuses on the method used for the estimation of free wavenumbers introduced by Ferguson et al. [8]. It is based on a correlation between measurements in the form of transfer functions and a wave considering trial wavenumbers, where the maxima indicate the wavenumber values present in the response. It was used by Souza et al. [9] to estimate the wavenumber of propagating waves in metamaterial beams and by El Masri et al. [10] in reinforced concrete beams. A similar correlation-based method was also presented by Berthaut et al. [11] where complex-valued trial wavenumbers were introduced along with directional flexibility and a scaling to restrict the correlation results to lie within the unity range. This method has been used in many works for the estimation of wavenumbers for varied types of structures ([12]).

In the current work, a numerical investigation using WFE is described in section 2. A unit cell of the real pipe is modelled and discretised to obtain the mass and stiffness matrices necessary for the calculation of wavenumbers. These results serve as reference and are supported by experimental observations, which are obtained through the correlation technique. The test setup and methodology are described in section 3, followed by implementation details for the experiments. Finally, section 4 contains a visual representation of how these two bending branches manifest in the mode shapes of the structure through the results of experimental and numerical modal analyses.

2 Numerical analysis

A 1D WFE approach is proposed to estimate the propagating wavenumbers of the helically grooved pipe. A periodic cell is modelled as a 11 mm long tube with cross-sectional dimensions extracted from a microscopic picture of a segment of the real structure. The 3D CAD model was meshed in Ansys Workbench 18.1 with different types of elements as with several levels of refinement until mesh convergence was achieved with a solid shell type of element with three solid shell elements through the thickness. The material properties were selected as the nominal values for stainless steel. The mesh of the model is shown in Fig. 1.

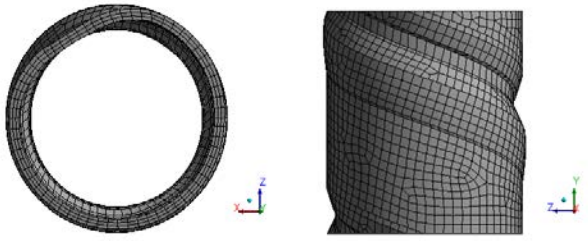

Fig. 1 - Meshed finite element model of a periodic cell of the helically grooved tube.

The FE model was used to extract the mass and stiffness matrices, $\boldsymbol{M}$ and $\boldsymbol{K}$, which compose the dynamic stiffness matrix $\boldsymbol{D} = \boldsymbol{K} - \omega^2 \boldsymbol{M}$. Damping was considered negligible. The equation of motion is expressed as

$$\boldsymbol{M}\ddot{\boldsymbol{q}} + \boldsymbol{K}\boldsymbol{q} = \boldsymbol{f} \tag{1}$$

where $\boldsymbol{f}$ and $\boldsymbol{q}$ are (2*n* x 1) vectors representing the loads and nodal displacement at the *n* DOFs on each side of the cell. It can be written in terms of the dynamic stiffness matrix $\boldsymbol{D}$ as

$$\boldsymbol{D}\boldsymbol{q} = \boldsymbol{f}. \tag{2}$$

Writing Eq. (2) in matrix form to reveal the association of the right or left nodes of the segment gives

$$\begin{bmatrix} \boldsymbol{D}_{LL} & \boldsymbol{D}_{LR} \\ \boldsymbol{D}_{RL} & \boldsymbol{D}_{RR} \end{bmatrix} \begin{Bmatrix} \boldsymbol{q}_L \\ \boldsymbol{q}_R \end{Bmatrix} = \begin{Bmatrix} \boldsymbol{f}_{\mathrm{L}} \\ \boldsymbol{f}_{\mathrm{R}} \end{Bmatrix}, \tag{3}$$

where the subscripts *L* and *R* discriminate between the left and right sides of the periodic cell (in this case, the top and bottom cross-section of the model shown in Fig. 1). The corresponding nodes from left and right sides can also be related through periodic conditions by defining a propagation constant λ, where the displacements and loadings are related through the expressions

$$\boldsymbol{q}_{\mathrm{R}} = \boldsymbol{\lambda}\, \boldsymbol{q}_{\mathrm{L}}, \boldsymbol{f}_{\mathrm{R}} = -\boldsymbol{\lambda}\, \boldsymbol{f}_{\mathrm{L}} \tag{4}$$

with

$$\lambda_j = e^{-jk_j\triangle} \tag{5}$$

where *k* is the unknown wavenumber, of which there are *n* solutions and △ is the length of the periodic cell. The internal nodes of the periodic cell were dealt with by performing a dynamic condensation.

Among the existing formulations for the WFE eigenproblem, the one used in this work can be reached by rewriting Eq. (3) with the substitutions from Eq. (4), and projecting the equations of motion onto the left-hand DOFs, leading to the eigenvalue problem ([13], [14]):

$$\left[\begin{bmatrix} \mathbf{0} & \boldsymbol{D}_{\mathbf{RL}} \\ -\boldsymbol{D}_{\mathbf{RL}} & -(\boldsymbol{D}_{\mathbf{LL}} + \boldsymbol{D}_{\mathbf{RR}}) \end{bmatrix} - \lambda \begin{bmatrix} \mathbf{D}_{\mathbf{RL}} & \mathbf{0} \\ \mathbf{0} & \mathbf{D}_{\mathbf{LR}} \end{bmatrix}\right] \begin{Bmatrix} \boldsymbol{q}_{\mathbf{L}} \\ \lambda\, \boldsymbol{q}_{\mathbf{L}} \end{Bmatrix} = \mathbf{0} \tag{6}$$

This eigenproblem has been reportedly useful for the estimation of free propagating waves in undamped waveguides ([14]). Numerical errors in the form of FE discretization error, round-off errors in the dynamic stiffness matrix and conditioning issues were verified in accordance to the guidelines from [14].

The handling of the stiffness and mass matrices into the eigenproblem of Eq. (6) and its solution were performed through a MATLAB script. The wavenumbers related to the free propagating waves were selected as the real-valued solutions from $k = -\ln \lambda/(i\Delta)$ and are also shown in Fig. 2. For reference, the wavenumbers resulting from the same analysis applied to a pipe without helical grooves but with otherwise identical geometry and material properties are shown in Fig. 2. Only the positive wavenumber axis is shown for simplicity. The main difference observed in this frequency range is the existence of two distinct flexural wavenumber branches, labelled $F(1,1)^+$ and $F(1,1)^-$ for the

helically grooved pipe. For the non-grooved tube, only one branch is visible, labelled $F(1,1)$ – or in fact two identical-valued branches representing the bending waveguide modes of degeneracy two in orthogonal directions of the pipe.

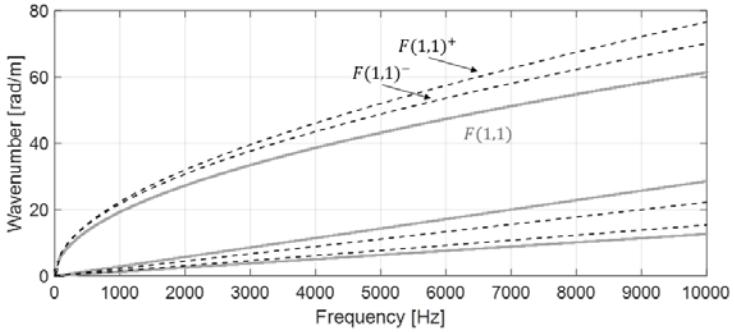

Fig. 2 - Predicted wavenumbers calculated through the WFE for the helically grooved tube (black dashed line) and for the non-grooved tube (grey continuous line).

The additional branches containing lower values of wavenumbers presented in Fig. 2 are for the torsional and longitudinal propagating waves and are not investigated experimentally in this work. In the following section of this paper, the experimental observations of the distinctive flexural branches in the dispersion curves of the helically grooved pipe are described.

3 Experimental investigation

The experimental approach to estimate wavenumbers considered herein is the correlation technique introduced by Ferguson [8]. It consists in finding, for each frequency, the wavenumber value that produces the maximum absolute value of the complex correlation function:

$$W(k_{tx}, k_{ty}, \omega) = \int_{-\infty}^{\infty} \int_{-\infty}^{\infty} w(x, y, \omega)\, e^{-jk_{tx}x} e^{-jk_{ty}y} dx dy \tag{7}$$

where the correlation of the measurements $w(x, y, \omega)$ with the wavefield $e^{-ik_{tx}x} e^{-ik_{ty}y}$ [for a 2D -plate] is evaluated. This can be assessed for any (k_{tx} k_{ty}) pair and these are designated as the trial wavenumbers. For a 1D waveguide with discrete measurement locations, Eq. (7) simplifies to:

$$\widehat{W}(k_{tx}, \omega) \approx \left(\frac{l_x}{N}\right) \sum_{i=1}^{N} w(x_i, \omega)\, e^{-jk_{tx}x_i}. \tag{8}$$

The correlation technique is an approach to convert the measured data from the spatial domain to the wavenumber domain, with the same purpose and in a fashion similar to that of a Spatial Discrete Fourier Transform (SDFT). In relation to the SDFT, the correlation technique has the advantage of having the wavenumber resolution determined arbitrarily by the user, which improves the estimation of wavenumbers for

a given dimension of the measurement grid ([8]). However, the energy leakage that exists in the SDFT is also present in the wavenumber spectrum generated by the correlation technique. It can affect the estimation of wavenumbers when they are closely spaced at a given frequency.

The measurements $w(x, \omega)$ are mobility functions measured along the length of the pipe with a roving hammer technique. The pipe was placed on a soft foam to simulate free boundary conditions. A laser Doppler vibrometer Polytec PDV100 was placed in a single location while an instrumented hammer PCB 086E80 excited 35 points (impact rover test), equally separated at a distance of 22 mm. The data was acquired and processed through the Data Physics Quattro data acquisition module along with its SignalCalc ACE software for signal processing.

Measurements for two pipes were made, one with and one without helical groove. Taking the non-grooved pipe as a reference and applying the correlation technique with the measured data, with trial wavenumbers ranging between ±100 rad/m and scaling each frequency step so that the maximum correlation amplitude is unitary led to the plot shown in Fig. 3a. Fig. 3b contains the plot with the dominant wavenumbers extracted from the colormap of Fig. 3a.

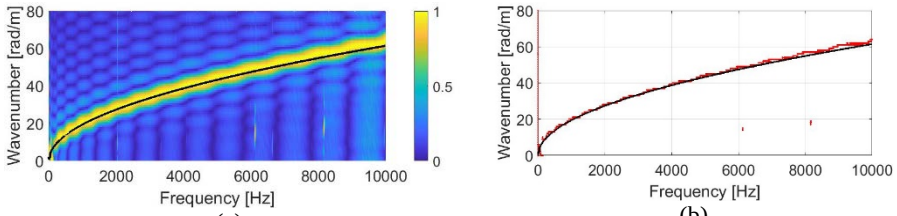

Fig. 3 - Predicted wavenumber with WFE (in black) versus estimated wavenumbers (in color) of the non-grooved pipe in (a) colormap of correlation and (b) extracted dominant wavenumbers.

The plots in Fig. 3 show that the predictions using WFE and the experimentally estimated wavenumbers are in good agreement and only one branch of the flexural mode is visible in the measured direction. The same procedure was applied to the helically grooved pipe, yielding the results shown in the plots of Fig. 4.

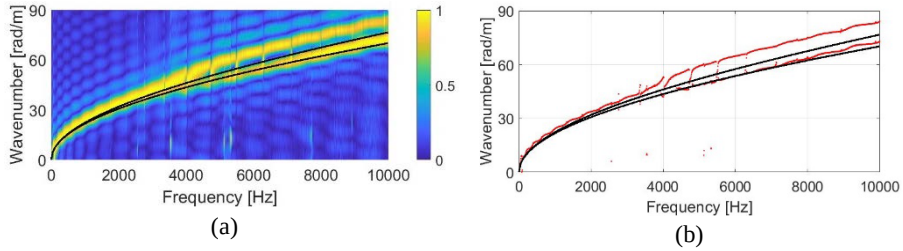

Fig. 4 - Predicted wavenumber with WFE (in black) versus estimated wavenumbers (in color) of the helically grooved pipe in (a) colormap of correlation and (b) extracted dominant wavenumbers.

From the numerical and experimental results, it is possible to observe two distinct branches in Fig. 4, though some quantitative disagreement exists. At frequencies below

4 kHz, the correlation technique is unable to distinguish two separate wavenumbers due to the leakage effect of converting the spatial samples into the *k*-space. Above 4 kHz, although two separate branches are discernible in the experimental results, there is some deviation in the results which could arise from differences in the material or geometrical properties used in the FE model.

Empirically, and inspired by the work of Manconi et al [1], it was observed that decreasing the Young's modulus of the grooved section of the pipe by a factor of 3 leads to a better fit between the results. This is shown in Fig. 5. Further investigation of the material properties in this structure would be necessary to make the numerical model more accurate, although this is not envisaged in this work.

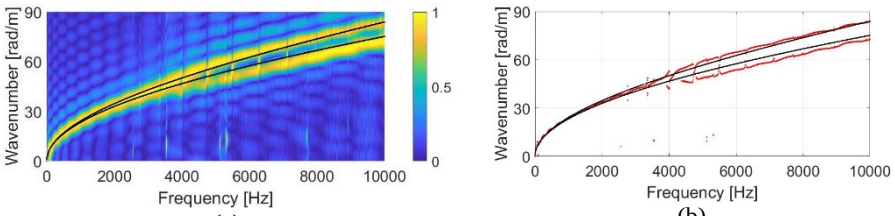

Fig. 5 - Predicted wavenumber with WFE (in black) versus estimated wavenumbers (in color) of the helically grooved pipe in (a) colormap of correlation and (b) extracted dominant wavenumbers.

4 The effect on the mode shapes due to the helical groove

The presence of the two distinctive flexural wave branches indicates potentially different mode shapes exist and this was analysed through an experimental modal analysis. The mobilities obtained previously were used and the experimental modal analysis performed along one direction of the pipes yielding the selected mode shapes shown in Fig. 6.

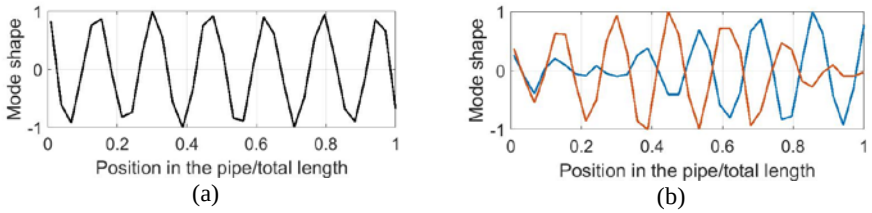

Fig. 6 - Mode shapes of the 12th order obtained experimentally for (a) the non-grooved pipe (at 5785 Hz and k=47.5 rad/m) and (b) the helically grooved pipe: two modes with varying magnitude at distinct and slightly different frequencies (4022 and 4042 Hz and $k \approx 47$ and 50.3 rad/m).

The mode shapes of the helically grooved pipe distinguish themselves from the ones of the non-grooved pipe through the change in magnitude at certain locations of each mode shape and through the existence of two mode shapes at slightly different frequencies for each mode order. Due to the one-directional view of the experimental modal analysis, a

numerical modal analysis performed in Ansys Workbench for a pipe with simplified helical groove is used to visualize the three-dimensional behaviour of the pipe.

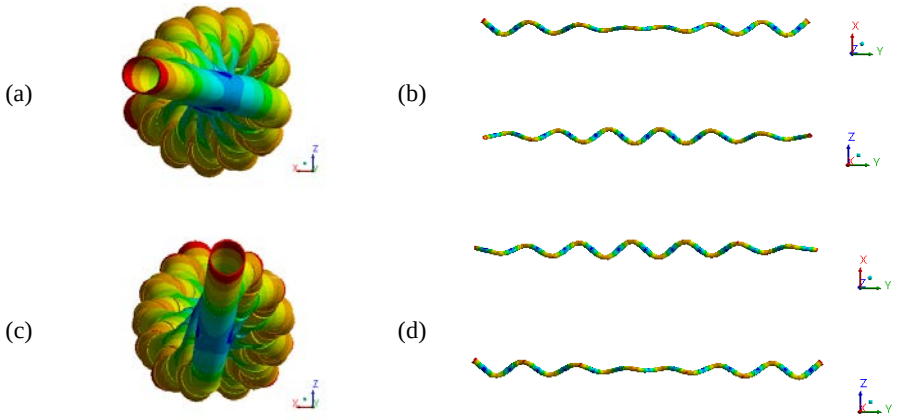

Fig. 7 – Two mode shapes of the helically grooved tube representing the 12th mode order: Mode 12-1 from it's (a) front view and (b) side views, Mode 12-2 (c) front view and (d) side views.

The mode shapes shown in Fig. 7 provide a clearer insight into the bending behaviour of the helically grooved tube. The fluctuations in magnitude that can be seen in Fig. 6b are explained in the side views of Fig. 7b and Fig. 7d as deflections that take place in a different direction than the one that was measured. The end result is a bending mode that is not restricted to lying in one direction only but occurs in a continuously rotating direction, as shown in Fig. 7a and 7c.

5 Conclusions

In this paper, the effect of a helical pattern on breaking degeneracy of the bending modes of a pipe has been shown experimentally. Both wave and modal approaches were investigated. The wavenumbers were initially estimated numerically through the WFE method and a real structure was tested with the correlation technique to estimate the wavenumbers experimentally. The excellent qualitative and quantitative agreement between the experimental and the numerical results corroborates the existence of two distinctive flexural branches. These contrast with the two identical branches existent on degenerate structures and are brought by the break of symmetry arising due to the helical pattern along the pipe. Mode shapes obtained experimentally and numerically evidence the effect of these distinctive propagating waves on the modal behaviour of the helically grooved pipe. The bending motion is seen not to be restricted to one fixed direction of the pipe for each mode (as it occurs for an axisymmetric pipe), but to a direction that continuously rotates along the length of the pipe.

Improvements can still be made on the material properties of the FE model for a more accurate representation of the effect of the manufacturing technique on the real structure.

Acknowledgements

This paper is supported by the European Union's Horizon 2020 research and innovation programme under the Marie Skłodowska-Curie grant agreement No 765636, project InDEStruct (Integrated Design of Engineering Structures).

References

1. Manconi, E., Sorokin, S., Garziera, R., Søe-Knudsen, A.: Wave Motion and Stop-Bands in Pipes with Helical Characteristics Using Wave Finite Element Analysis, Journal of Applied and Computational Mechanics, vol. 4, pp. 420-428, (2018).
2. Treyssède, F., Laguerre, L.: Investigation of elastic modes propagating in multi-wire helical waveguides, Journal of Sound and Vibration, vol. 329, pp. 1702-1716, (2010).
3. Treyssède, F.: Numerical investigation of elastic modes of propagation in helical waveguides, The Journal of the Acoustical Society of America, vol. 121, no. 6, pp. 3398-3408, (2007).
4. Liu, Y., Han, Q., Li, C., Huang, H.: Numerical investigation of dispersion relations for helical waveguides using the Scaled Boundary Finite Element method, Journal of Sound and Vibration, vol. 333, pp. 1991-2002, (2014).
5. Frikha, A., Treyssède, F., Cartraud, P.: Effect of axial load on the propagation of elastic waves in helical beams, Wave Motion, vol. 48, pp. 83-92, (2011).
6. Renno, J. M., Mace, B. R.: Vibration modelling of helical springs with non-uniform ends, Journal of Sound and Vibration, vol. 331, no. 12, pp. 2809-2823, (2012).
7. Demma, A., Cawley, P., Lowe, M., Pavlakovic, B.: The Effect of Bends on the Propagation of Guided Waves in Pipes, Journal of Pressure Vessel Technology, vol. 127, no. 3, pp. 328-335, (2005).
8. Ferguson, N. S., Halkyard, C. R., Mace, B. R., Heron, K. H.: The estimation of wavenumbers in two-dimensional structures, in Proceedings of Isma 2002: International Conference on Noise and Vibration Engineering, Vols 1-5, pp. 799-806, (2002).
9. Souza, M. R., Beli, D., Ferguson, N. S., de F. Arruda, J. R., Fabro, A. T.: A Bayesian approach for wavenumber identification of metamaterial beams possessing variability, Mechanical Systems and Signal Processing, vol. 135, p. 106437, (2020).
10. El Masri, E., Ferguson, N., Waters, T.: Wave propagation and scattering in reinforced concrete beams, The Journal of the Acoustical Society of America, vol. 146, pp. 3283-3294, (2019).
11. Berthaut, J., Ichchou, M., Jézéquel, L.: Wavenumbers identification in two-dimensional structures: Comparison between two new methods, in Proceedings of the Tenth International Congress on Sound and Vibration, pp. 1155-1162, (2003).
12. Ichchou, M. N., Berthaut, J., Collet, M.: Multi-mode wave propagation in ribbed plates: Part I, wavenumber-space characteristics, International Journal of Solids and Structures, vol. 45, no. 5, pp. 1179-1195, (2008).
13. Cicirello, A., Mace, B. R., Kingan, M. J., Yang, Y.: Sensitivity analysis of generalised eigenproblems and application to wave and finite element models, Journal of Sound and Vibration, vol. 478, p. 115345, (2020).
14. Waki, Y., Mace, B., Brennan, M.: Numerical issues concerning the wave and finite element method for free and forced vibrations of waveguides, Journal of Sound and Vibration, vol. 327, pp. 92-108, (2009).